# LOW CYCLE FATIGUE STRENGTH OF X65 PIPELINE GIRTH WELDS

Gotoh, Koji
Department of Marine Systems Engineering, Kyushu University

Berge, Stig
Department of Marine Structures, Norwegian University of Science and Technology



出版情報：pp.1653-1660, 2004-10-04. American Society of Mechanical Engineers: ASME
バージョン：

**Proceedings of IPC 2004**
**International Pipeline Conference**
**October 4 – 8, 2004 Calgary, Alberta, Canada**

# IPC04-0631

# LOW CYCLE FATIGUE STRENGTH OF X65 PIPELINE GIRTH WELDS

Koji Gotoh
Department of Marine Systems Engineering
Kyushu University
Fukuoka, Japan

Stig Berge
Department of Marine Structures
Norwegian University of Science and Technology
Trondheim, Norway

## ABSTRACT

During pipe laying at large water depth using S-lay over a stinger, the pipe may be subjected to reversed plastic strains which could lead to low cycle fatigue failure. X65 pipeline girth welds with wall thickness 22mm were tested in cyclic strain control. Undermatched and overmatched welds were tested. Two types of cyclic strain programs were applied. In the first test series the welds were subjected to a tensile-tensile cyclic strain, simulating pipe going over the stinger, to validate that a pipe going over a stinger would not violate criteria for low cycle fatigue design. In the second test series, the specimens were initially pre-strained to 2% and subsequently fatigue-cycled with a maximum strain of 2% to obtain design criteria for a pipe laying stationary over the stinger for a period of time, subjected to cyclic loads due to waves. The results are presented in terms of $\Delta\varepsilon - N$ curves, with proposed design curves for the two types of welds.

## INTRODUCTION

The most cost-efficient laying method for offshore pipelines is S-lay, Figure 1. S-lay has been applied in laying of a large majority of pipelines (diameter larger than 16 inches) in the North Sea. With the S-lay method, pipe sections are joined at welding stations on the deck of the vessel. The pipe is deployed over a stinger structure with rollers, to provide a smooth and controlled curvature of the pipe. The pipe is fed over the stinger into the sea by moving the vessel forwards on its anchors.

The departure angle $\varphi$ is essentially a function of the submerged weight of the pipe and coating, and the available force capacity of the anchor system. The stinger is vulnerable to wave loading, and for most of the larger laying vessels the stinger length cannot be extended further. An increase in departure angle must therefore be accommodated by an increased curvature of the stinger. Hence, the curvature and applied strain to a pipe during laying is essentially determined by the departure angle.

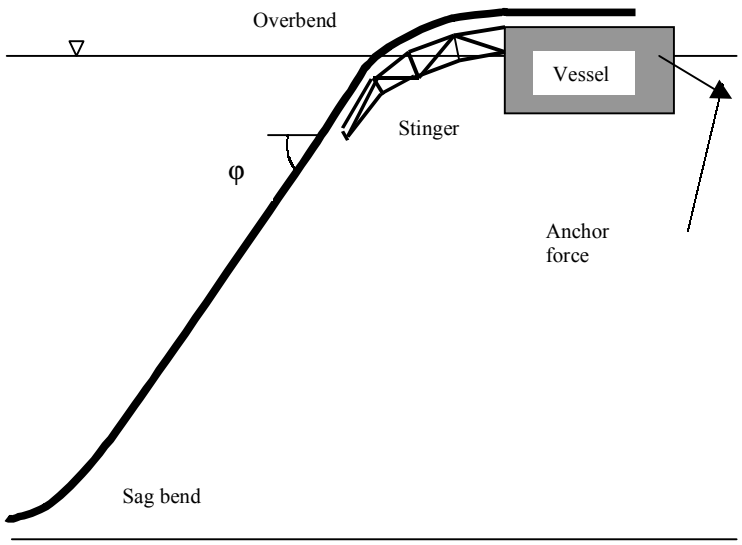


Figure 1. S-lay of offshore pipelines

For current pipelines at water depth of 300 – 500 m the nominal strain in the pipe wall during laying is limited to essentially elastic conditions. For deep water pipelines (1500 - 2000 m water depth) using the current generation of laying vessels, the departure angle may be approaching $90^o$ due to limited force capacity of the anchor system. In this situation, considerable plastic strains may develop during pipe laying. It should be recognised that the pipe is loaded in a displacement or strain controlled situation. A more detailed discussion on limiting factors for deep water pipe laying was presented by Damsleth et al. (1999).

## FATIGUE CONSIDERATIONS

For a pipe subjected to large plastic strains during laying, two scenarios need to be considered from a fatigue design point of view. Firstly, the strain range that is applied during laying should not violate fatigue strength requirements for reversed loading. According to the fatigue clauses of the Norwegian Petroleum Directorate (1992) primary structure shall be designed with a utilisation factor of 10 on fatigue life. The implication is that for the maximum strain range the design SN curve for the weld should be at least 10 cycles.

Secondly, due to operational reasons (e.g. problems at welding stations and similar) the laying may become interrupted, and the pipe in the overbend section may be exposed to fatigue loading from waves. In this case the pipe has been pre-bent to a certain level of strain, which must be taken into account in a fatigue assessment.

There have been several studies concerning fatigue strength of girth welded steel pipes. Buitrago and Zettlemoyer (1998) discussed the development of fatigue design criteria for critical girth welded components, and proposed $S-N$ curves based on re-evaluation of recent, large-scale fatigue data. Maddox and Razmjoo (1998) carried out fatigue tests on large-scale girth welded pipes and small-scale strips cut from girth welded pipes and butt welded plates, to assess the influence of weld quality and joint misalignment, and to compare the fatigue performance of small-scale and large-scale specimens. However, the target of these studies was high-cycle and stress controlled fatigue problems for pipes in the installed condition, and SN curves were given in terms of stress range. There seems to be no established criteria for fatigue design of pipelines subjected to cyclic plastic strains.

In this paper low cycle fatigue tests on X65 pipeline girth welds are reported. The tests were carried out on coupon specimens, cut from girth welded pipes with wall thickness 22 mm. Undermatched and overmatched welds were tested. Two types of cyclic strain programs were applied. The results are presented in terms of $\Delta\varepsilon-N$ curves, with proposed design curves for the two types of welds.

## EXPERIMENTAL

Material properties of pipe material grade X65 are shown in Table 1. Hour-glass shaped specimens were cut longitudinally from X65 pipeline girth welded pipes with wall thickness 22 mm, length 2000 mm and diameter 406 mm (16 inches). The specimens were sectioned by a water jet abrasive cutting method. This cutting method leaves a smooth surface with no heat affected zone. The fatigue strength of the surface cut by water jet is superior to the strength of as-rolled surface; i.e. the surface did not affect the fatigue strength of the specimens. The width of the specimens in the test section was 40 mm. Specimen geometry is shown in Figure 2.

Overmatched and undermatched welded specimens were tested. The tests were carried out in the as-welded state. To investigate the properties of weld material, cross weld tensile testing was performed. The test results are shown in Table 2. As shown, the amount of overmatch was approximately 10%, whereas the undermatch was marginal, due to the variability of base material yield strength.

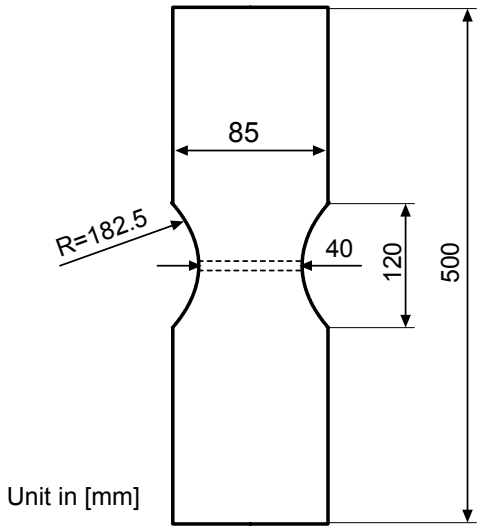


Figure 2. Specimen geometry.

The fatigue failures of overmatched specimens were consistently located in the base metal and the ones of undermatched specimens were located in the weld metal.

The test procedure complied with ASTM E606 (1992). The specimens were hydraulically clamped using shaped clamps made from steel, Figure 3. Loading was applied axially, using a ±1 MN servo-hydraulic actuator in strain control.

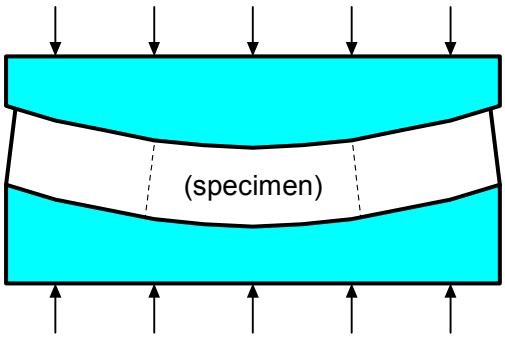


Figure 3. Clamping of specimens in hydraulic grips.

Two types of cyclic strain programs were applied. In Series 1 the welds were tested with a zero-tensile pulsating strain, simulating pipe going over the stinger. The objective of this test was to validate that a pipe going over a stinger would not violate criteria for low cycle fatigue design. In Series 2 the specimens were initially pre-strained to 2.0%, which was monotonic tensile, and subsequently fatigue cycled with a

maximum strain of 2.0 % to obtain $\Delta\varepsilon - N$ curves. The objective of this test was to obtain design criteria for a pipe laying stationary over the stinger for a period of time, subjected to cyclic loads due to waves.

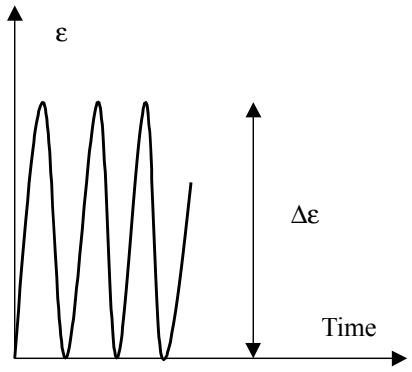


Figure 4. Load program simulating pipe going over stinger.

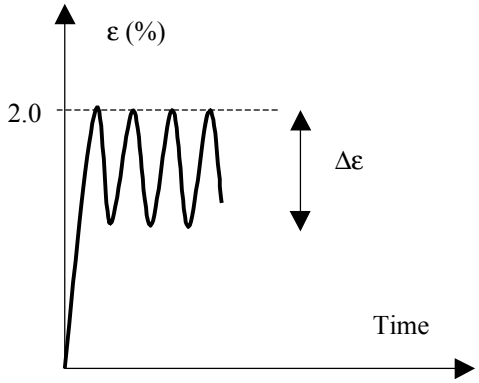


Figure 5. Load program simulating pipe lying over stinger and subjected to wave loading.

Strain was measured using an extensometer with gauge length 50 mm, symmetrically located over the weld. This averaged strain was assumed to represent a nominal strain in the pipe wall. Load and strain were continuously logged during the tests.

The tests were performed at ambient temperature. A thermo-couple was attached to each specimen at the test cross section. The cycling rate was controlled so that the temperature of the specimen would never exceed 50 $^{o}$C to avoid any significant change of material properties due to heating.

During testing the specimens were monitored visually to observe any tendency for buckling. No such tendency was observed.

## TEST RESULTS

According to the ASTM standard for low cycle fatigue testing, several criteria of failure may be defined. In this study, two failure criteria were employed. One was defined visible crack initiation, where the crack size was equal to about 2 mm. The other was defined by a 50 % load drop. It turned out that the former definition was the most conservative criterion.

Examples of hysteresis loops are shown in Figures 6 - 8. Figure 6 shows an example from Series 1. Three different curves are shown in this figure. The dotted line represents the initial (first five cycles) hysteresis loops. The bold solid line represents the loop at visible crack initiation. The fine solid line represents the loop at 50 % load drop. As shown in Figure 6 the material had a tendency towards cyclic softening. At 50 % load drop, a point of inflection is clearly displayed in the hysteresis loop. This inflection point indicates the onset of crack closure and a corresponding increase in stiffness.

Figure 7 shows an example from Series 2. Three different curves are shown also in this figure. The dotted line shows the initial load history, with the monotonic pre-strain to 2 % and the following 10 cycles with a maximum strain of 2 %. The bold and fine solid lines represent the same as in Figure 6. Cyclic softening and crack closure were easily identified at 50 % load drop. The similarity of Figures 6 and 7 with regard to cyclic behaviour is apparent, indicating that the 2% prestrain of Series 2 had no significant effect on the subsequent cyclic strain behaviour.

In Figure 8 is shown an example of hysteresis loops from Series 1, at a relatively small strain range. The cyclic softening is apparent also in this case.

Test results are shown in Tables 3 and 4, and in Figures 9 and 10 plotted on the basis of $\Delta\varepsilon - N$.

As shown in Figures 9 and 10, the data fall within a relatively narrow scatter band for each type of weld. There is no significant difference between the data obtained with the two load programs. The data were therefore pooled together and analysed by regression analysis to give the following mean life $\Delta\varepsilon - N$ curves.

Overmatched welds:

$$\Delta\varepsilon = 8.308 \cdot N^{-0.3258} \quad \text{Visible crack initiation} \quad (1)$$

$$\Delta\varepsilon = 8.453 \cdot N^{-0.3032} \quad \text{50\% load drop} \quad (2)$$

Undermatched welds:

$$\Delta\varepsilon = 10.95 \cdot N^{-0.4142} \quad \text{Visible crack initiation} \quad (3)$$

$$\Delta\varepsilon = 11.24 \cdot N^{-0.3705} \quad \text{50\% load drop} \quad (4)$$

## DISCUSSION

### Definition of fatigue life

As shown in Figures 9 and 10, there was some difference between two definitions of fatigue life; life to surface crack initiation being more conservative. For overmatched welds (Figure 9) the difference is hardly significant compared to the overall scatter. For undermatched welds (Figure 10) the difference is somewhat larger, still the residual life after visual crack detection (initiation) was less than the number of cycles to initiation. For assessment of SN design curves, cycles to crack initiation was selected.

### Effect of weld metal

Overmatched and undermatched welded specimens were tested in the as-welded state. In all the overmatched welded specimens, fatigue crack initiation and growth took place in the base metal, close to the fusion line. In the undermatched welds fatigue initiation and growth took place in the weld metal.

Comparing the two types of welds, the fatigue strength is essentially the same for large cyclic strains. Due to different slopes of the two ε-N curves overmatched welds have a somewhat larger fatigue strength overall.

### Proposed design curve

In Figures 11 and 12 the results of Figures 9 and 10 are shown more in detail, with regression lines defining mean life curves and scatterband defined by a shift by one and two standard deviations of $\log N$ on either side of the mean curve (mean $\pm s$, mean $\pm 2s$). As noted above there is no significant difference between the data obtained with the two load programs and most of the data fall within the band of two standard deviations.

Following the normal procedure for structural fatigue design, design curves are proposed on the basis of mean life minus two standard deviations, based on visual crack initiation. The following formulae were derived:

Overmatched welds:

$$\Delta\varepsilon = 5.734 \times N^{-0.3258} \quad (5)$$

Undermatched welds:

$$\Delta\varepsilon = 7.647 \times N^{-0.4142} \quad (6)$$

In Figures 11 and 12 these design curves are shown in bold lines (lower bold lines).

## CONCLUSIONS

Pipe laying at large water depth using S-lay over a stinger may cause plastic deformation of the pipe. In this study, low cycle fatigue strength of X65 pipeline girth welds, which were undermatched and overmatched, was tested in cyclic strain control. Cyclic strain range was varied between 0.5 and 2.0. The following conclusions were drawn:

1. Monotonic pre-strain to 2% prior to cyclic straining had no significant effect on fatigue strength.

2. For overmatched welds, fatigue initiation and crack growth took place in base material, close to the fusion line. For undermatched welds cracks were initiated and would grow in weld metal.

3. At large cyclic strains there was no significant difference in fatigue strength of the two types of welds. At smaller strain ranges overmatched welds had a somewhat larger fatigue strength compared to undermatched welds.

4. Fatigue life to initiation of a visible surface crack was shorter than life to 50% load drop.

5. Fatigue design curves based on life to visible crack initiation, was proposed on the basis of mean life minus two standard deviations. The curves are based on fatigue life data in the range 100 – 50.000 cycles.

## AKNOWLEDGEMENTS

This work was carried out as part of the DEEPIPE project, by SINTEF (project leader), Det Norske Veritas and JP Kenny. The project was supported by the Norwegian Research Council, UK Health and Safety Executive, Statoil, Conoco, Phillips, Allseas, ETPM and Mannesmann Röhr. Financial and technical support is gratefully acknowledged.

## REFERENCES

ASTM, 1992. " Standard Practice for Strain-Controlled Fatigue Testing", Designation: E 606-92.

Buitrago, J. and Zettlemoyer, N., 1998, "Fatigue Design of Critical Girth Welds for Deepwater Applications", OMAE98-2004.

Damsleth, P. Bay, Y. Nystrøm P. R. and Gustafsson C. (1999), “Deepwater Pipeline Installation with Plastic Strain”, OMAE99-5046.

Maddox, S.J. and Razmijoo, G.R., 1998. "Fatigue Performance of Large Girth Welded Steel Tubes", OMAE98-2355.

Norwegian Petroleum Directorate, Regulations relating to loadbearing structures in the petroleum activity, 1992.

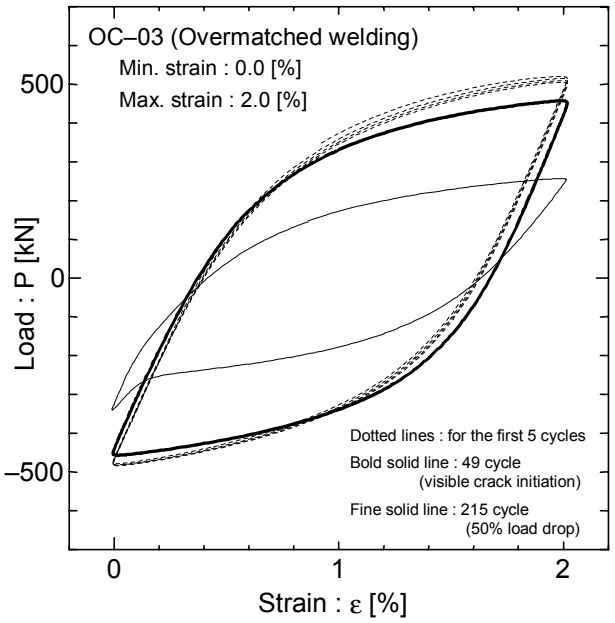


Figure 6. Hysteresis loops for Series 1, zero-tensile loading, 2% strain range, cf. Figure 4.

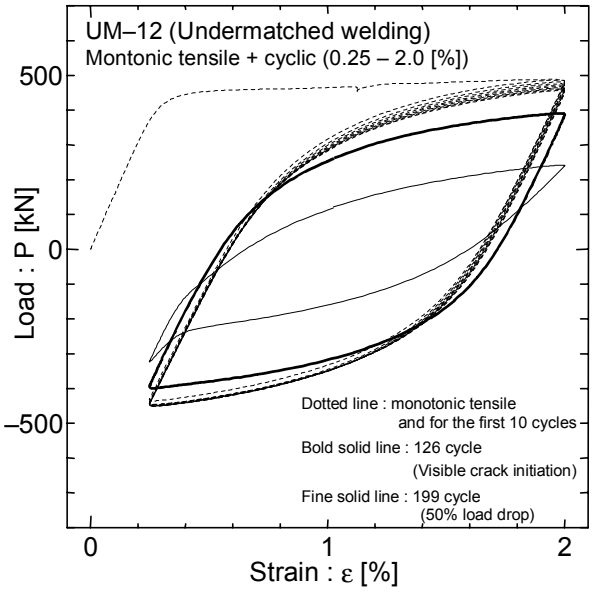


Figure 7. Hysteresis loops for Series 2, 2% maximum strain, 1.75% strain range, cf. Figure 5.

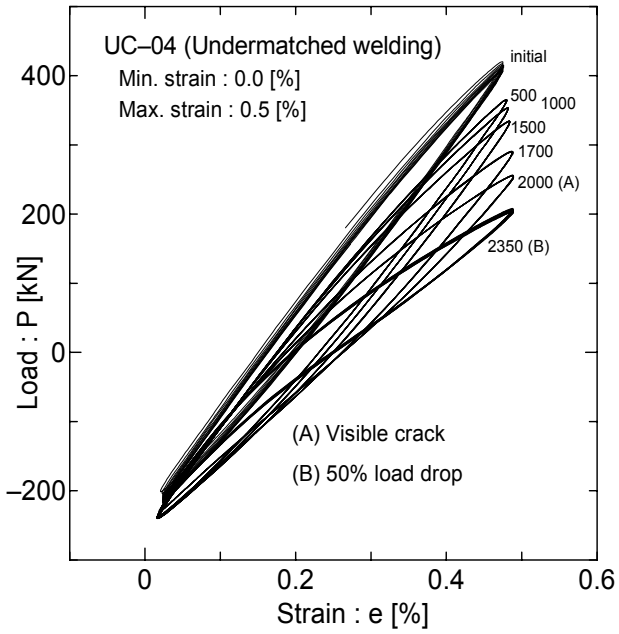


Figure 8. Hysteresis loops for Series 1, zero-tensile strain, 0.5% strain range, cf. Figure 4.

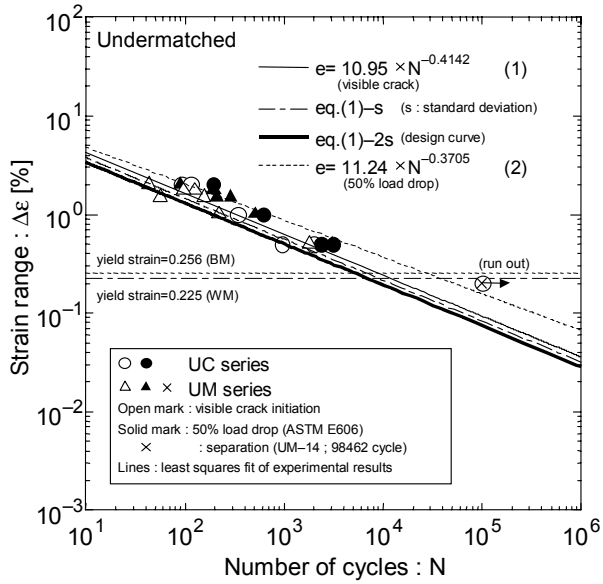


Figure 9. ε-N data for overmatched welds, regression analysis based on first visible crack and 50% load drop respectively.

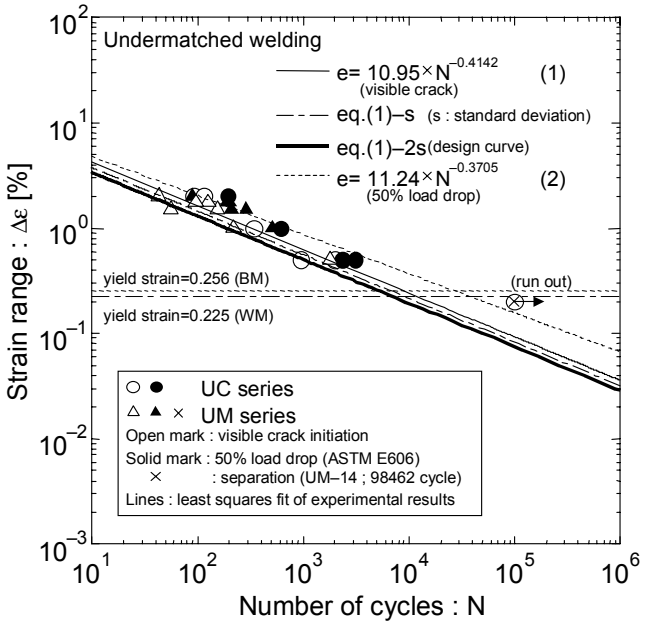


Figure 10. ε-N data for undermatched welds, regression analysis based on first visible crack and 50% load drop respectively.

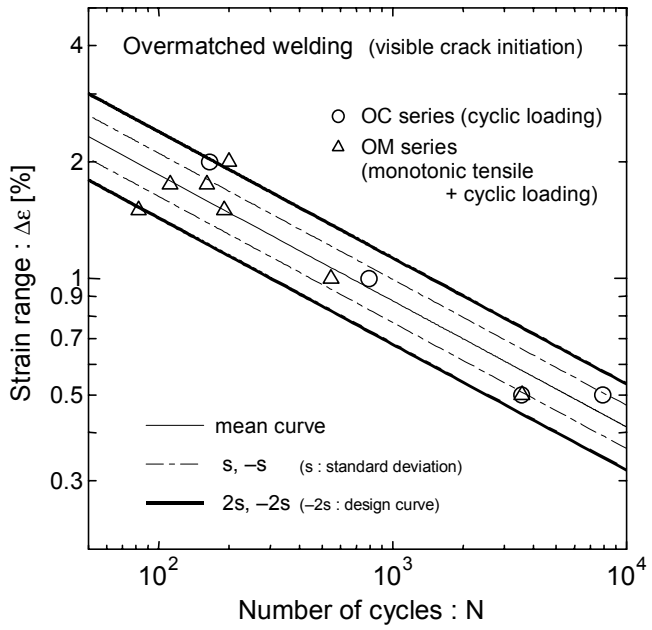


Figure 11. ε-N data for overmatched welds, regression analysis based on first visible crack.

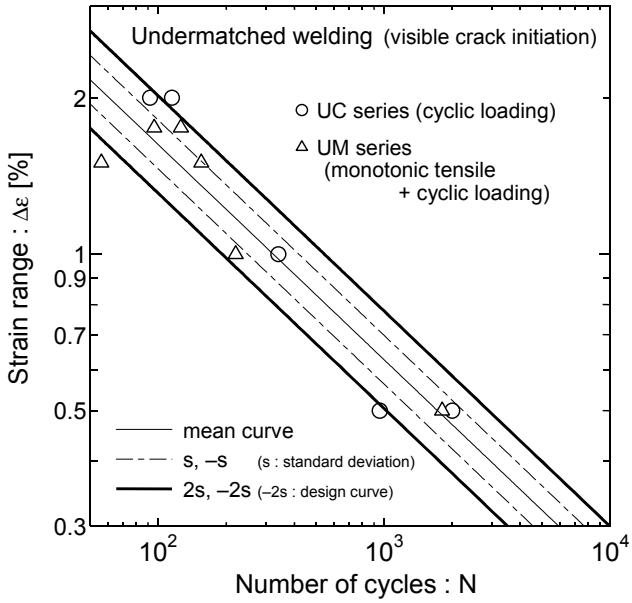


Figure 12. ε-N data for undermatched welds, regression analysis based on first visible crack.

Table 1 Material properties

| End of pipe | Yield stress (MPa) | Tensile strength (MPa) | Elongation (%) |
|---|---|---|---|
| Jet side | 487 | 593 | 28.0 |
| End side | 513 | 626 | 27.0 |

Table 2 Results of cross weld tensile tests with cylindrical specimens

| weld type | Diameter (mm) | Upper yield strength (MPa) | Lower yield strength (MPa) | True stress at max. load (MPa) | Equivalent strain at max. load | Equivalent fracture strain |
|---|---|---|---|---|---|---|
| overmatched | 6,01 | 539 | 505 | 677 | 0,11 | 1,44 |
| overmatched | 6,02 | 527 | 493 | 669 | 0,10 | 1,45 |
| undermatched | 6,03 | 517 | 513 | 720 | 0,16 | 1,01 |
| undermatched | 6,01 | 514 | 511,0 | 724 | 0,17 | 1,05 |

Table 3. Test data for overmatched welds.
OC – zero-tensile cyclic loading (Series 1, cf. Figure 4)
OM – 2% tensile pre-strain, cyclic loading with maximum strain 2% (Series 2, cf. Figure 5)

| Specimen | Strain range (%) | N (visible crack) | N (50% load drop) | N (other) | Comment |
|---|---|---|---|---|---|
| OC-01 | 0.0-2.0 | | | 21 | Fracture |
| OC-02 | 0.0-2.0 | 165 | 243 | | |
| OC-03 | 0.0-2.0 | 49 | 215 | | |
| OC-04 | 0.0-0.5 | 7.899 | 10.700 | | |
| OC-05 | 0.0-0.5 | 3.560 | 6.500 | | |
| OC-06 | 0.0-0.2 | | | 100.000 | Run-out |
| OC-07 | 0.0-1.0 | 791 | 1.134 | | |
| OM-09 | 0.0-2.0 | 200 | 291 | | |
| OM-10 | 0.5-2.0 | 82 | 304 | | |
| OM-11 | 0.5-2.0 | 191 | 362 | | |
| OM-12 | 0.25-2.0 | 161 | 308 | | |
| OM-13 | 0.25-2.0 | 112 | 239 | | |
| OM-14 | 1.8-2.0 | | | 100.000 | Run-out |
| OM-15 | 1.0-2.0 | 546 | 824 | | |
| OM-16 | 1.5-2.0 | 3.565 | 5.814 | | |

Table 4. Test data for undermatched welds.
UC – zero-tensile cyclic loading (Series 1, cf. Figure 4)
UM – 2% tensile pre-strain, cyclic loading with maximum strain 2% (Series 2, cf. Figure 5)

| Specimen | Strain range (%) | N (visible crack) | N (50% load drop) | N (other) | Comment |
|---|---|---|---|---|---|
| UC-01 | 0.0-2.0 | 92 | 115 | | |
| UC-04 | 0.0-0.5 | 2.000 | 2.350 | | |
| UC-05 | 0.0-0.5 | 955 | 3.117 | | |
| UC-06 | 0.0-2.0 | 115 | 194 | | |
| UC-07 | 0.0-0.2 | | | 100.000 | Run-out |
| UC-08 | 0.0-1.0 | 340 | 615 | | |
| UM-09 | 0.0-2.0 | 43 | 90 | | |
| UM-10 | 0.5-2.0 | 56 | 208 | | |
| UM-11 | 0.5-2.0 | 155 | 290 | | |
| UM-12 | 0.25-2.0 | 126 | 199 | | |
| UM-13 | 0.25-2.0 | 96 | 189 | | |
| UM-14 | 1.8-2.0 | | | 98.462 | Fracture |
| UM-15 | 1.0-2.0 | 220 | 512 | | |
| UM-16 | 1.5-2.0 | 1.806 | 3.073 | | |